Structural and Magnetic Properties of bcc Phase Fe90−xMn10Alx (x = 10, 20, 30, and 40) Nanocrystalline Alloys

by Kontan Tarigan

Journal of the Korean Physical Society, Vol. 62, No. 12, June 2013, pp. 1969~1973

Structural and Magnetic Properties of bcc Phase $Fe_{90-x}Mn_{10}Al_x$ (x = 10, 20, 30, and 40) Nanocrystalline Alloys

Kontan TARIGAN
Department of Electrical Engineering, Indonesia Institute of Technology, Serpong-Tangerang Selatan 15320, Indonesia

Young Yeal SONG and Seong-Cho YU*
Department of Physics, Chungbuk National University, Cheongju 361-763, Korea

Dwi NANTO
Physics Education, Syarif Hidayatullah State Islamic University, Jakarta 15412, Indonesia

(Received 5 June 2012, in final form 21 September 2012)

Nanocrystalline $Fe_{90-x}Mn_{10}Al_x$ (x = 10, 20, 30, and 40) were prepared via mechanical alloying by using Fe, Mn, and Al powders with a 48 hours milling time. The structural and the magnetic properties were studied. All X-ray diffraction peaks are broader and shifted to smaller angle with increasing Al contents, depending on the crystalline size and the lattice parameter. All the samples exhibit alloys behavior with an average crystallite size around 10 nm. The magnetic saturation, coercivity, and permeability obtained from measurements using a vibrating sample magnetometer showed strong dependences on the Al content and these dependences were related to changes in the structure and the crystallite size. The hyperfine field obtained from Mössbauer spectroscopy varied with the Fe content. These results suggest that, by adjusting Al, appropriate magnetization values can be obtained without affecting the coercivity and the structure of the bcc phase.

PACS numbers: 61.66.Dk, 61.47.-w
Keywords: Nanocrystalline, Mechanical alloying, FeMnAl
DOI: 10.3938/jkps.62.1969

I. INTRODUCTION

A wide range of applications for amorphous and nanocrystalline magnetic materials arises because of the versatile nature of those materials, which can provide fast magnetization reversal with minimal magnetic losses [1, 2]. Fe-Mn-Al alloys are of technical and scientific interest because many different properties appear depending upon the concentration and the heat treatment. In fact, these alloys can be prepared in crystalline, quasicrystalline and amorphous states. Especially, the magnetic properties depend very strongly on the crystalline structure, the phase composition, and the degree of order in such alloys [3]. Due to the presence of competitive and diluted exchange interactions, they can exhibit different magnetic phases, such as paramagnetic, ferromagnetic, spin-glass, reentrant spin-glass and anti-ferromagnetic phases [4,5]. Fe-Mn-Al alloys in the bcc-disordered phase have been intensively studied both theoretically and experimentally owing to different magnetic phases appearing as a consequence of variations in the composition and in the temperature [6].

In 1977, Chakrabarti studied the disordered Fe-Mn-Al alloy system and obtained a structural phase diagram by using X-ray diffraction [7]. Those alloys were obtained by melting in an arc furnace and afterwards by heating them to 1000 °C and quenching them in iced water. The results showed a stable austenitic phase (FCC) at low Al concentration and Mn concentrations below 60 at.%. Some researchers found that the system was antiferromagnetic, that the behavior was diluted by increasing the Fe and the Al contents, and that the alloys become paramagnetic when the Fe content was over 70 at.% [8,9]. A few studies on the ternary Fe-Mn-Al systems obtained by mechanical alloying (MA) have reported the effects of varying Mn or Al concentration the structural properties, *i.e.*, the crystalline structure, the lattice parameter, and on the grain size [10]. Rebolledo *et al.* reported that the Fe-Mn-Al system has magnetic and structural properties similar to those exhibited by powders of melted alloys with the same composition in general, especially when they had been mechanically alloyed for long times [10]. The magnetic properties of FeMnAl alloys were reported in a single $Fe_{55}Mn_{10}Al_{35}$ composition as a function of milling time in our previous work [11]. Systematic

*E-mail: scyu@cbnu.ac.kr

works, however, on the Fe-Mn-Al alloys are required to understand the structural and the magnetic properties.

We prepared nanocrystalline $Fe_{90-x}Mn_{10}Al_x$ (x = 10, 20, 30, and 40) alloys by using MA with a milling time of 48 hours and studied their structural and magnetic properties. Their structural and magnetic properties were then studied by using X-ray diffraction (XRD), scanning electron microscopy (SEM), Mössbauer spectroscopy and vibrating sample magnetometer (VSM).

II. EXPERIMENTS

Nanocrystalline $Fe_{90-x}Mn_{10}Al_x$ (x = 10, 20, 30, and 40 at.%) alloys were prepared by using the MA method with a high-energy planetary ball mill SPEX 8000 mixer with stainless-steel balls and a stainless-steel vial at a speed of 1425 rpm. The starting mixture of the samples was formed by using commercial powders of Fe (Im-3m, 53 μm, 99.9%), Mn (I-43m, 75 μm, 99.9 %), and Al (fm-3m, 53 - 106 μm, 99.9%). For the milling, the weight ratio of the balls-to-powder mixture was 5:1. The $Fe_{90-x}Mn_{10}Al_x$ alloys were mixed and ground with a milling time of 48 hours. This process was performed in an Ar ambience to avoid oxidation.

After the preparation, the sizes and the morphologies of the particles were checked preliminarily by using SEM. The magnetic measurements were carried out by using VSM with a maximum field of 1.5 T at room temperature. The XRD data were obtained by using an X-ray diffractometer with Cu-Kα radiation. The alloy samples were also investigated by using Mössbauer measurements at room temperature with a conventional constant acceleration spectrometer in the transmission geometry. The hyperfine structure was then refined by fitting with the MOSFIT program [12].

III. RESULTS AND DISCUSSION

Figure 1 shows typical SEM images with a magnification of 100k and reveal the variation in the particle shape and the size of the nano-crystalline $Fe_{90-x}Mn_{10}Al_x$ (x = 10, 20, 30, and 40 at.%) alloys after 48 hours of milling. Our SEM study reveals that the particles present in the samples have quite similar shapes, with very small particles being located on the surfaces of big particles. There are large particles or agglomerates with spherical shapes. The particle sizes varied as we changed the Al content. The average particle sizes estimated from the SEM images decreased with increasing Al content.

XRD patterns obtained from the nanocrystalline $Fe_{90-x}Mn_{10}Al_x$ alloys are shown in Fig. 2. The three top curves show the XRD patterns of the elements of a pure crystalline sample for comparison. After milling, the peak intensities of Al and Mn disappeared. The amorph

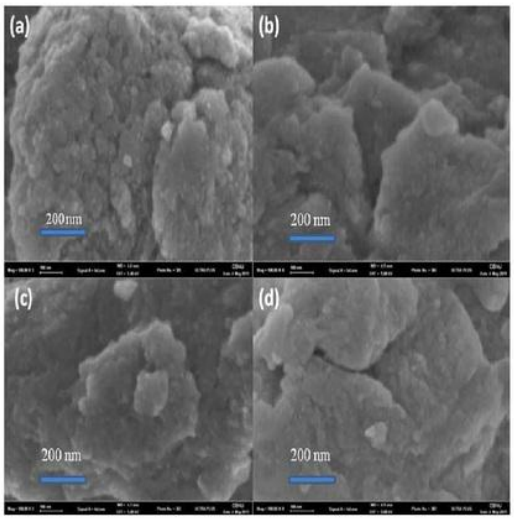

Fig. 1. (Color online) Typical SEM images of nanocrystalline $Fe_{90-x}Mn_{10}Al_x$ alloys with (a) x = 10, (b) x = 20, (c) x = 30, and (d) x = 40 at.%.

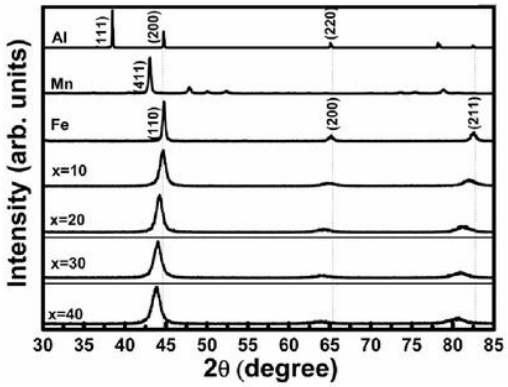

Fig. 2. XRD patterns of mechanically-alloyed nanocrystalline $Fe_{90-x}Mn_{10}Al_x$ (x = 10, 20, 30, and 40 at.%) alloys.

process of Al and Mn can be assumed to have occurred, of the Fe structure starts undergoing fracture and welding during repeated milling. The four curves below show the progress of the solid-state reaction of the $Fe_{90-x}Mn_{10}Al_x$ (x = 10, 20, 30, and 40 at.%) system during MA with milling for 48 hours. All the $Fe_{90-x}Mn_{10}Al_x$ peaks are broader and shifted to smaller angles, which is due to the deformation of the structure and the variation in the crystallite size. The deformation is due to the replacement Fe atoms by Al and Mn atoms as defects caused by large local strains in the powder particles, which is a signal for the formation of an alloy. One can also see that all the peaks have the same trend belonging to the bcc phase structure. Furthermore, the peak positions

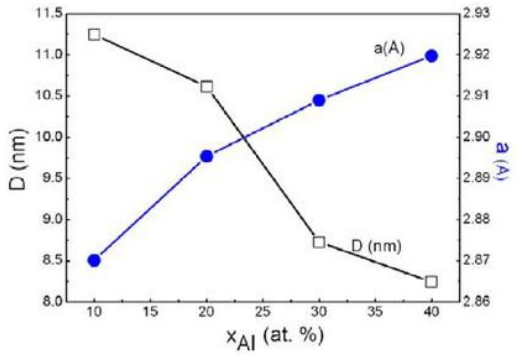

Fig. 3. (Color online) Crystallite size and lattice parameter of nanocrystalline $Fe_{90-x}Mn_{10}Al_x$ alloys as functions of the Al content.

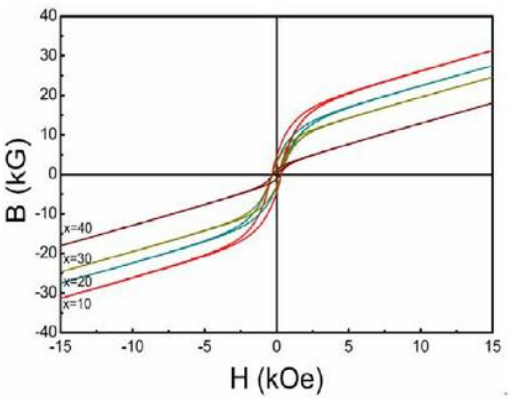

Fig. 4. (Color online) Typical hysteresis loops of nanocrystalline $Fe_{90-x}Mn_{10}Al_x$ (x = 10, 20, 30, and 40 at.%) alloys.

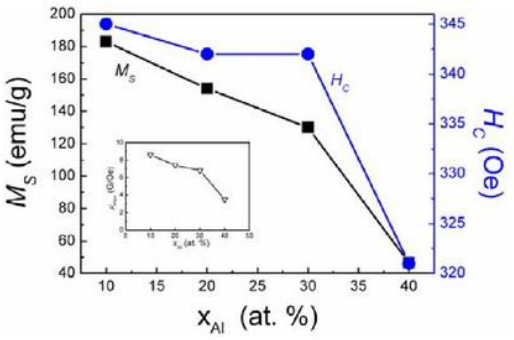

Fig. 5. (Color online) Variations of the magnetic saturation, coercivity, and permeability of nanocrystalline $Fe_{90-x}Mn_{10}Al_x$ alloys with the Al content.

shift slightly toward lower angle upon partial substitution of Al and Mn for Fe-site, indicating an increase in the lattice parameter based on Bragg's law.

The crystallite size and the lattice parameter, based on Fe (110) peaks, with respect to the Al content for the $Fe_{90-x}Mn_{10}Al_x$ (x =10, 20, 30, and 40 at.%) system, are shown in Fig. 3. Based on the XRD data the crystallite size (D) can be evaluated from the Scherrer formula $D = 0.9\lambda/(B\cos\theta_B)$, where λ is the X-ray wavelength (1.5406 Å), θ_B the diffraction angle at the peak, B the full width at half maximum (FWHM). The lattice parameter can be evaluated from Bragg condition $nd = 2d_{hkl}\sin\theta$, where d_{hkl} is the distance between atomic layers in a crystal plan hkl, and n an integer. In this case, $d_{hkl} = a/(h^2 + k^2 + l^2)^{1/2}$. As a result, the estimated crystallite size is around 8 to 11 nm and the lattice parameter is around 2.87 to 2.92 Å. The variations of the crystallite size and the lattice parameter based on Fe (110) peak with respect to the Al content are reasonable. The changes in crystal size and internal strain have been examined by using X-ray diffraction on powder samples for different Al contents. The crystallite size decreases as the Al content is increased, being around 11 nm at $x = 10$ and around 8 nm at $x = 40$ at.%. Accordingly, the lattice parameter increases as the Al content is increased because it is related to the larger atomic size of the Al atoms in comparison to those of the Fe and the Mn atoms.

The magnetic behaviors can be found from the $M-H$ graph and can be modified to the $B-H$ graph as shown in Fig. 4. The magnetic saturation (M_s), the coercivity (H_c), and the permeability (μ_{max}) found from the hysteresis loop depend strongly on the Al content. Figure 5 shows that the M_s, H_c, and μ_{max} decrease as the Al content is increased. Based on XRD for all compositions, we see that the Al and the Mn atoms are diffused into the Fe structure. Variations of these quantities could come from a decrease in crystallite size and a dilution of the magnetic Fe lattice with increasing Al content. Grains of $Fe_{90-x}Mn_{10}Al_x$ occurred in the mono-domain region. The permeability can be obtained indirectly by using the relation $B(\mathrm{G}) = H(\mathrm{Oe}) + 4\pi M(\mathrm{emu/cm^3})$, where B is magnetic induction, H the magnetic field and M the magnetization in a unit volume. The gradients (B/H) yield the maximum permeability (μ_{max}) values as shown in the inset to Fig. 5. The μ_{max} value decreases with increasing Al content, being around 9 G/Oe at $x = 10$ at.% and around 3.5 G/Oe at $x = 40$ at.%.

Room-temperature Mössbauer measurements taken at different compositions allowed us to observe the alloy formation, as shown in Fig. 6. For the lowest Fe content, that is, $Fe_{50}Mn_{10}Al_{40}$, a singlet spectrum and a positive isomer shift ($\delta \approx 0.067$) without a hyperfine field was detected. This spectrum is similar to that in the work of with Rico *et al.* on $Fe_{40}Mn_{30}Al_{30}$, which means that at lower Fe content in the Fe-Mn-Al system, the Mössbauer spectra (MS) has a singlet spectrum. One can find with increasing Fe content, a significant change in MS. The starting $Fe_{60}Mn_{10}Al_{30}$ hyperfine field distribution has a

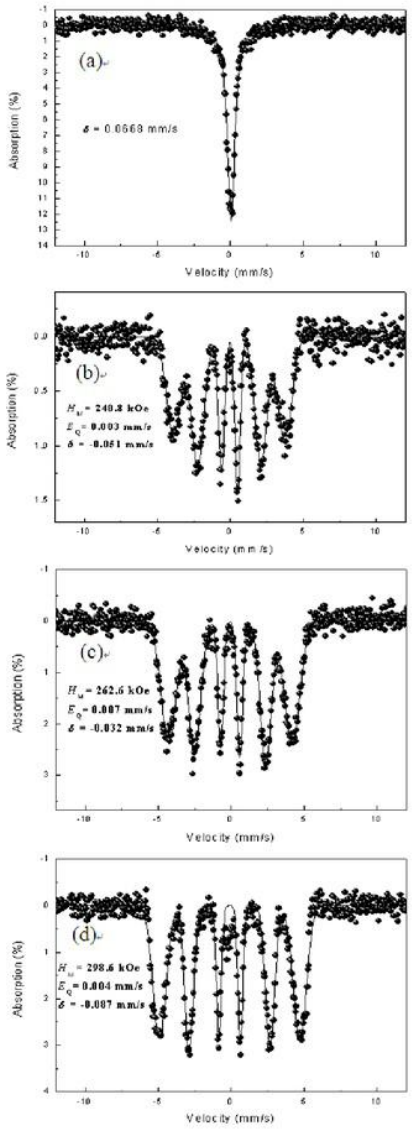

Fig. 6. Mössbauer spectra of nanocrystalline $Fe_{90-x}Mn_{10}Al_x$ with (a) $x = 40$, (b) $x = 30$, (c) $x = 20$, and (d) $x = 10$ of at.% measured at room temperature.

sextet structure and all negative isomer shifts correspond to the bcc Fe phase, similar to other previous work reported by Rebolledo [10]. The MS for various Fe contents show various line broadenings due to diffusion of the Al and the Mn into Fe matrix. Increasing Fe content implies a broadened line spectra and increasing hyperfine field. The hyperfine field from the MS gives information on the Fe sites surrounded with other Fe nearest neighbors (nn). Higher Fe content has more Fe nn, as confirmed by the broader line spectra, while lower Fe content has fewer Fe nn. The spectra changes dramatically, becoming a singlet spectrum at the lowest Fe content. Even the evolution of the MS shows evidence for an Fe - Fe interaction corresponding to the magnetization; however, the alloy structure remains stable in the bcc phase.

IV. CONCLUSION

We can conclude that the $Fe_{90-x}Mn_{10}Al_x$ ($x = 10$, 20, 30, and 40 at.%) samples produced by mechanical alloying present a ferromagnetic behavior for different Al contents. We suggest that the structures of all the samples are of the bcc type and that the elements Mn and Al replace the Fe atoms, as explicitly shown by the XRD peaks of $Fe_{90-x}Mn_{10}Al_x$. The M_s, H_c and μ_{max} were significantly changed when the Al content was changed. Therefore, we may control the Al content to obtain appropriate M_s, H_c and μ_{max} values. Mössbauer spectroscopy gives local magnetic information around Fe and showed that increasing the Fe content resulted in a higher hyperfine and a broader line. Wide applications of magnetic material based on the Fe-Mn-Al system have drawn attention to the Al content. In this work, we demonstrated that the Al content played an important role in the magnetization with a stable coercivity. As a structural study, our work showed that there were no changes in structure even for large Al contents.

ACKNOWLEDGMENTS

This research was supported by the converging Research Center Program funded by the Ministry of Education Science and Technology (Grant 2012K001431), South Korea.

REFERENCES

[1] R. Hasegawa, J. Magn. Magn. Mater. **215-216**, 240 (2000).
[2] R. Hasegawa, J. Magn. Magn. Mater. **304**, 187 (2006).
[3] H. Bremers, M. Fricke and J. Hesse, Hyperfine. Interact. 1855 (1994).
[4] M. M. Rico, L. E. Zamaro, G. A. Perez Alcazar, J. M. Gonzalez and A. Hernando, Jr., Phys. Stat. Sol. (b) **220**, (2000).
[5] J. Restrepo, G. A. Perez Alcazar and J. M. Gonzalez, J. ppl. Phys. **87**, 7425 (2000).
[6] M. M. Rico, G. Medina, G. A. Pérez Alcazar, J. S. Munoz, S. Surinach and M. D. Baro, Phys. Stat. Sol. **189**, 811 (2002).
[7] D. J. Chakrabarti, Metal. Trans. B **8**, 121 (1977).

[8] R. R. Rodréguez J., G. A. Pérez Alcazar and H. S. Chepa, Phys. Stat. Sol. (c) **2**, 3597 (2005).
[9] G. A. Perez Alcazar, J. A. Plascak and E. Galvao da Silva, Phys. Rev. B **38**, 2816 (1988) .
[10] A. F. Rebolledo, J. J. Romero, R. Cuadrado, J. M. Gonzalez, F. Pigazo, F. J. Palomares, M. H. Medina and G.A. Pérez Alcazar, J. Magn. Magn. Mater. **316**, e-418 (2007).
[11] K. Tarigan, Y. G. Yoo, D. S. Yang, J. M. Grenéche and S. C. Yu, IEEE Trans. Magn. **45**, 2492 (2009).
[12] F. Varret and J. Teillet, "MOSFIT Program," Université du Maine, France.

Structural and Magnetic Properties of bcc Phase Fe90−xMn10Alx (x = 10, 20, 30, and 40) Nanocrystalline Alloys

ORIGINALITY REPORT

16%	9%	14%	%
SIMILARITY INDEX	INTERNET SOURCES	PUBLICATIONS	STUDENT PAPERS

PRIMARY SOURCES

1	R. R. Rodríguez J., G. A. Pérez A., H. Sánchez Sthepa. "Time milling and composition effects on the magnetic and structural properties of the FexMn0.95-xAl0.05 (0.40 Publication	1%
2	Heiko Bremers. "Structure and magnetic properties of FeMnAl alloys investigated by Mössbauer spectroscopy and X-ray diffraction", Hyperfine Interactions, 12/1994 Publication	1%
3	www.mse.buaa.edu.cn Internet Source	1%
4	J. Restrepo, G.A. Pérez Alcázar, J.M. González. "Room Temperature Magnetic Properties of the Mechanically Alloyed Fe0.8—xMnxAl0.2 System", physica status solidi (b), 2000 Publication	1%
5	aclweb.org Internet Source	1%

6	T. V. S. M. Mohan Babu. "Mössbauer effect in atomic ordered and disordered Fe0.75−xMnxAl0.25 alloys", physica status solidi (b), 01/01/1996 Publication	1%
7	www-lab.imr.tohoku.ac.jp Internet Source	1%
8	Zamora, L.E.. "Mossbauer and magnetization evidence of spin-glass phase in the Fe"0"."4"5Mn"0"."2"5Al"0"."3"0 disordered alloy", Journal of Magnetism and Magnetic Materials, 19941101 Publication	1%
9	Nanto, Dwi, Seong-Cho Yu, Suhk-Kun Oh, Nikolay Chebotaev, and Andrey Telegin. "Influence of A -Site Deficiency on Magnetocaloric Effect in Nonstoichiometric $({\rm La}_{0.8}{\rm Ca}_{0.2})_{0.975}{\rm MnO}_{3.01}$ ", IEEE Transactions on Magnetics, 2014. Publication	1%
10	bibliotecadigital.udea.edu.co Internet Source	1%
11	"Table of contents", IEEE Transactions on Magnetics, 2009. Publication	1%

12	onlinelibrary.wiley.com Internet Source	1%
13	Bae, J.S.. "Crystallinity and morphology dependent luminescence of Li-doped Y"2"-"xGd"xO"3:Eu^3^+ thin film phosphors", Applied Surface Science, 20060430 Publication	1%
14	nanojournal.ifmo.ru Internet Source	1%
15	Hasegawa, R.. "Magnetic inductor based on nanosize amorphous metal powder", Journal of Non-Crystalline Solids, 20070415 Publication	1%
16	Hasegawa, R.. "Advances in amorphous and nanocrystalline magnetic materials", Journal of Magnetism and Magnetic Materials, 200609 Publication	1%
17	Azzaza, S., S. Alleg, and J. J. Suñol. "Phase Transformation in the Ball Milled $Fe_{31}Co_{31}Nb_8B_{30}$ Powders", Advances in Materials Physics and Chemistry, 2013. Publication	<1%
18	Lucila I. Doumic, Gabriel Salierno, Cinthia Ramos, Patricia M. Haure, Miryan C. Cassanello, María A. Ayude. ""Soluble" vs. "insoluble" Prussian blue based catalysts:	<1%

	influence on Fenton-type treatment", RSC Advances, 2016 Publication	
19	Won-Tae Kim. "Mossbauer spectroscopy studies in supersaturated Fe/sub x/Co/sub 50-x/Cu/sub 50/ solid solutions", IEEE Transactions on Magnetics, 1997 Publication	<1%
20	hal.archives-ouvertes.fr Internet Source	<1%
21	A. Osorio. "Theoretical study of Fe-Mn-Al alloys in the fcc disordered phase", Physical Review B, 04/1996 Publication	<1%
22	Slodicka, M.. "Numerical study of nonlinear ferromagnetic materials", Applied Numerical Mathematics, 200307 Publication	<1%
23	nanoscalereslett.springeropen.com Internet Source	<1%
24	www.sim.utcluj.ro Internet Source	<1%
25	darwin.bth.rwth-aachen.de Internet Source	<1%
26	J. Restrepo, J. M. González, G. A. Pérez Alcázar. "Monte Carlo study of the magnetic	<1%

properties of Fe-rich Al–Fe disordered alloys", Journal of Applied Physics, 1997
Publication

27	Mark J. Dekkers, Martin A. A. Schoonen. " Magnetic properties of hydrothermally synthesized greigite (Fe S)-I. Rock magnetic parameters at room temperature ", Geophysical Journal International, 1996 Publication	<1%
28	baadalsg.inflibnet.ac.in Internet Source	<1%

Exclude quotes	Off	Exclude matches	Off
Exclude bibliography	Off		